JACS
JOURNAL OF THE AMERICAN CHEMICAL SOCIETY
pubs.acs.org/JACS
Article

Avoidance of Secondary Carbocations, Unusual Deprotonation, and Nonstatistical Dynamic Effects in the Cyclization Mechanism of Tetraisoquinane

Xiuting Wei, William DeSnoo, Zining Li, Wenbo Ning, Wang-Yeuk Kong, Jordan Nafie, Dean J. Tantillo,* and Jeffrey D. Rudolf*

Cite This: J. Am. Chem. Soc. 2025, 147, 16293−16300
Read Online
ACCESS | Metrics & More | Article Recommendations | Supporting Information

ABSTRACT: The complexity and versatility of terpene cyclization reactions contribute to the wide variety of functions and properties that terpenoid compounds exhibit in nature. The management of reactive carbocations over the course of the reaction to ultimately arrive at a particular carbon fragment connectivity and stereochemistry is no small feat. Bacteria possess a variety of TSs that generate diverse polycyclic terpene skeletons; however, terpenoids in myxobacteria are especially rare. Here, we report the first mechanistic study of tetraisoquinene biosynthesis from TiqS, a diterpene synthase from *Melittangium boletus*. To understand formation of the unique 5/5/5/5-fused tetraisoquinane skeleton, we used the isolation and structural elucidation of nine minor metabolites, site-directed mutagenesis, stable isotope labeling experiments, and quantum chemical calculations to propose and support its mechanism. This study reveals a new mechanism of diterpene cyclization, expands our understanding of terpenoid biosynthesis, and enables the discovery of novel natural products in myxobacteria.

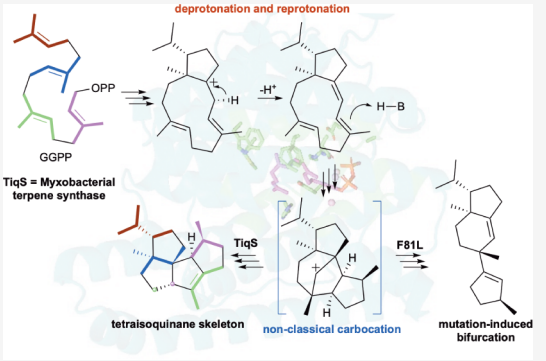

INTRODUCTION

Over 100,000 terpenoids are known in nature, making the terpenoids the most structurally diverse family of natural products.[1] Many of these compounds, or their synthetic derivatives, are used as scents, flavors, or pharmaceuticals.[1−5] Despite the expansive skeletal library of the terpenome, genome mining, particularly in microbes, continues to lead to the discovery of novel terpene skeletons. Our recent work using genome mining to identify and characterize new terpene synthases (TSs) in bacteria expanded the known chemical space of the hydrocarbon skeletons that bacteria produce.[6] In that study, we identified several new diterpene skeletons that were previously unknown in nature.

Tetraisoquinene (**1**), a novel 5/5/5/5-fused tetracyclic skeleton with six stereocenters, is produced by TiqS, a TS from the myxobacterium *Melittangium boletus* DSM 148713. Structurally, the closest known carbon skeleton to **1** is tetraquinane (hence our naming of **1**), a similar 5/5/5/5 ring system with differing connectivity of the A and B rings, found in the fungal crinipellins. Crinipellins, first isolated in 1979 from *Crinipellis stipitaria*, are the only known tetraquinane natural products and exhibit antibacterial and anticancer properties.[7,8] Due to their structural uniqueness and biological activities, they have been successful targets of total synthetic efforts.[9−14] Conversely, there is no firm understanding of the biosynthetic origins of the crinipellins or their tetraquinane skeleton. There are no TSs known that form the tetraquinane skeleton and no biosynthetic pathway for the crinipellins has been characterized. As we identified the first TS known to produce the tetraisoquinane skeleton, we sought to elucidate the cyclization mechanism of TiqS.

The arrangement of isoprene units in a terpene skeleton is essential in proposing its cyclization mechanism. The proposed cyclization mechanism for the tetraquinanes was recently proposed (Figure S1)[14] and with the exception of a single methyl shift, all four isoprene units appear to be easily identified (Figure 1). For **1**, however, all four isoprene units are not obvious based on the skeleton alone, indicating carbon rearrangement during TiqS catalysis. In this study, we propose a cyclization mechanism for **1** based on varied sources of evidence, including the isolation and structural elucidation of minor metabolites, site-directed mutagenesis, stable isotope labeling experiments, and quantum chemical calculations. These calculations support the presence of a post-transition state bifurcation that involves passage through a nonclassical carbocation that is essential to the formation of **1**. In addition,

Received: January 29, 2025
Revised: April 16, 2025
Accepted: April 17, 2025
Published: April 29, 2025

https://doi.org/10.1021/jacs.5c01828
J. Am. Chem. Soc. 2025, 147, 16293−16300

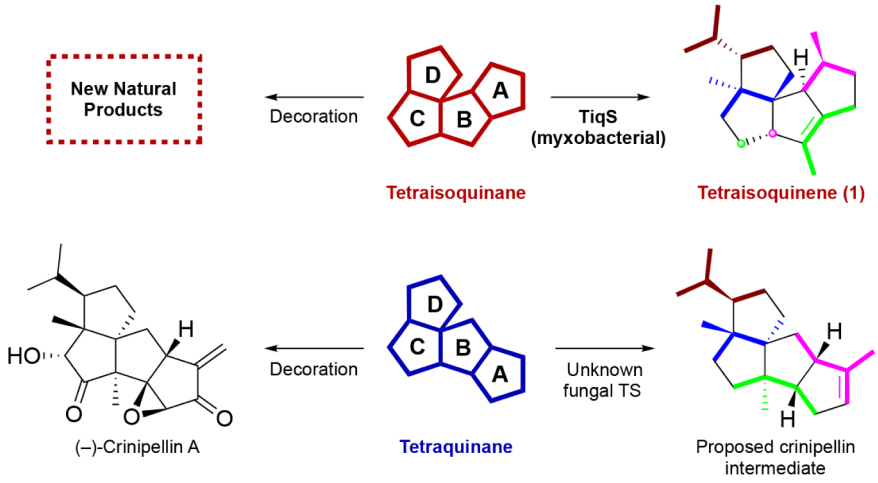

Figure 1. Tetraisoquinane and tetraquinane diterpenes: core skeletons, proposed isoprene units, and natural products. In this study, the cyclization mechanism of the novel tetraisoquinane skeleton by TiqS, a myxobacterial diterpene synthase, is elucidated. Tetraquinane, the known skeleton in the crinipellin family of fungal natural products, has a different A–B ring system. The four proposed isoprene units are colored in brown, blue, green, and magenta. No enzymes, neither TS or decoration enzymes, are known for the biosynthesis of the tetraquinane skeleton or the crinipellins.

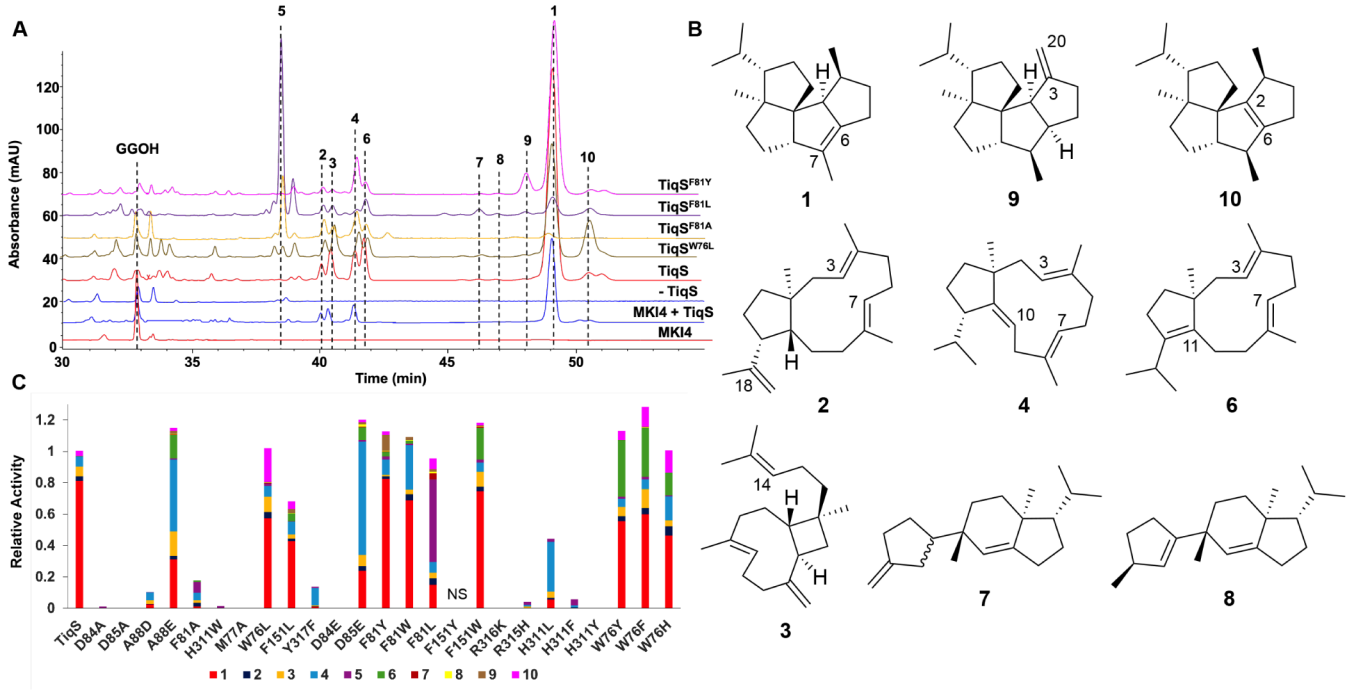

Figure 2. Native TiqS and its variants produce 10 diterpenes with five distinct skeletons. (A) HPLC analysis of wild-type TiqS in vitro and in an *E. coli* strain engineered for GGPP overproduction (MKI4). Hydrolyzed GGPP (GGOH) and isolated diterpenes **1**–**10** are labeled. Compounds were detected by UV (λ = 210 nm). (B) The structures of **1**–**10** (see SI for structural elucidation and spectroscopic data). Diterpenes **1**–**4** were produced by wild-type TiqS in MKI4; **5**–**10** were isolated from various active site mutants. (C) Relative production of **1**–**10** from TiqS and 25 active site variants. Areas under the curve (λ = 210 nm) for **1**–**10** were individually calculated and their sum was set to 1 in TiqS. NS; not soluble.

several shunt products, isolated from both native TiqS and its variants, themselves contain novel diterpene skeletons.

RESULTS AND DISCUSSION

Characterization of TiqS and Its Minor Products Reveals First Key Steps of Tetraisoquinene Biosynthesis. The major product of TiqS (UniProt: A0A250IBE0) is **1**, seen in both an engineered *Escherichia coli* strain (MKI4) for geranylgeranyl diphosphate (GGPP) production and an in vitro reaction with GGPP.[6] To test if TiqS was active using farnesyl diphosphate (FPP) or geranylfarnesyl diphosphate (GFPP) as substrates, we expressed *tiqS* in *E. coli* strains engineered for FPP (MKI3) and GFPP (MKI5) production. No C_{15} or C_{25} products were detected by HPLC supporting TiqS as a diterpene-specific TS (Figure S2). In both in vitro reactions and heterologous expression in the MKI4 system, TiqS produced several additional diterpenes (**2**–**4**; Figure 2A). A 12-L fermentation of TiqS in the MKI4 system was conducted to isolate **1**–**4**. The tetraisoquinene structure of **1** was confirmed by NMR and MS spectroscopy analysis (Table S4, Figs. S3–S5). Using 1D and 2D NMR, the planar skeletons of **2**–**4** were determined to be xeniaphyllene (**3**), the 4/9-

https://doi.org/10.1021/jacs.5c01828
J. Am. Chem. Soc. 2025, 147, 16293–16300

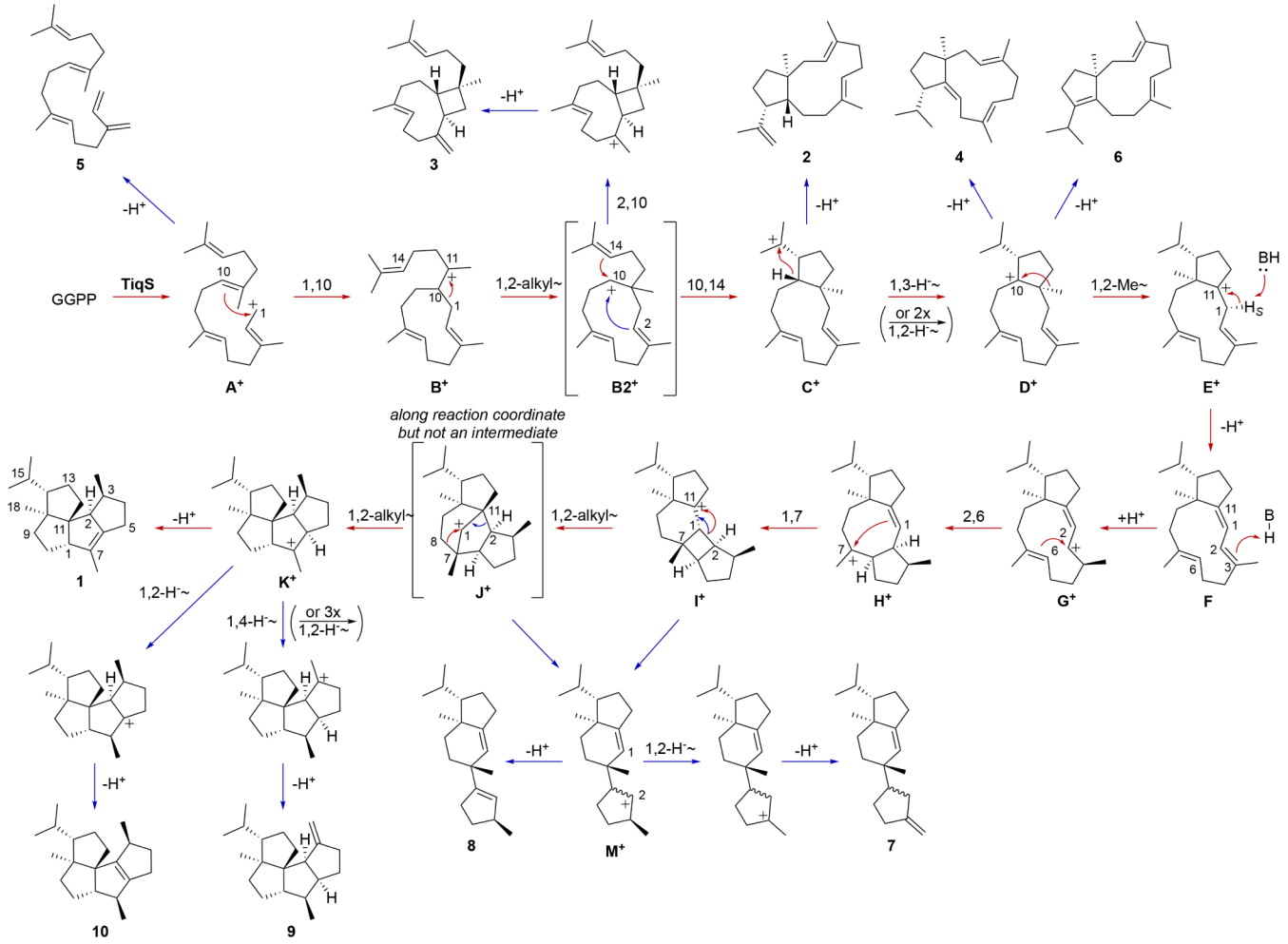

Figure 3. Proposed cyclization mechanism of tetraisoquinene by TiqS. Main cyclization pathway (red arrows) from GGPP to **1** are supported by isolated compounds, deuterium labeling experiments, and quantum chemical calculations. Shunt pathways to **2**–**10** (blue), supporting the mechanism to **1**, are shown.

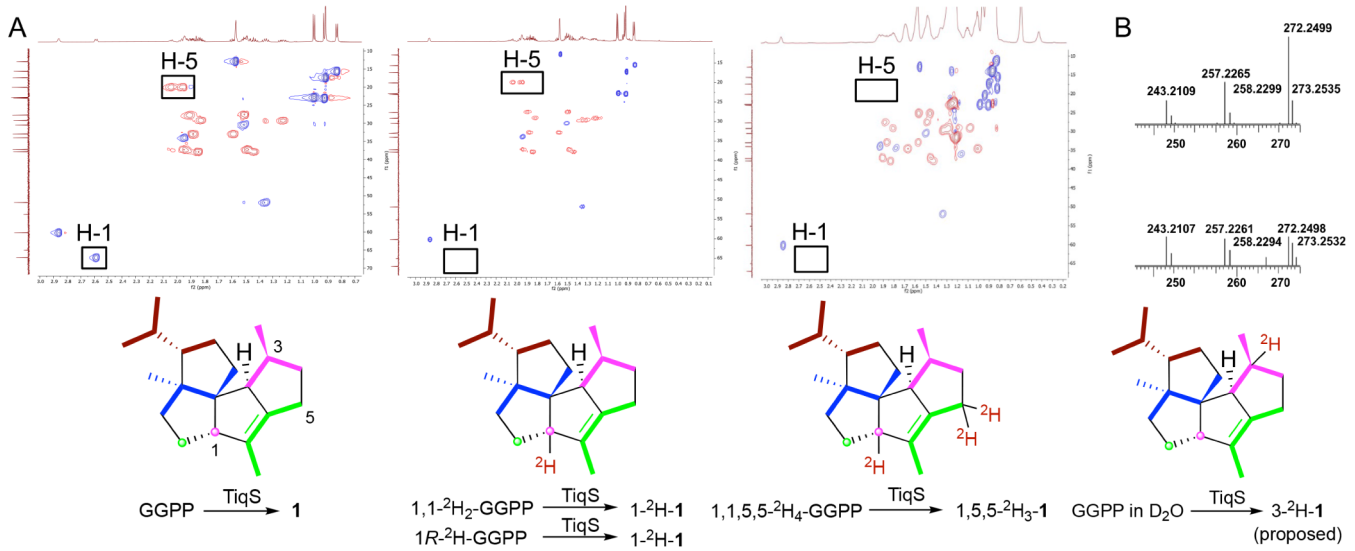

Figure 4. Deuterium-labeled GGPP supports isoprene units and C-1 rearrangement. (A) Incubation of TiqS with unlabeled GGPP, 1,1-$^2H_2$-GGPP, 1*R*-^{2}H-GGPP, and1,1,5,5-$^2H_4$-GGPP gave **1**, 1-^{2}H-**1**, 1-^{2}H-**1**, and 1,5,5-$^2H_3$-**1**, respectively. Zoomed-in ^{1}H−^{13}C HSQC spectra of **1**, 1-^{2}H-**1**, 1-^{2}H-**1**, and 1,5,5-$^2H_3$-**1** in benzene-d_6 are shown above each structure. (B) Incubation of TiqS with unlabeled GGPP in D_2O increased the molecular weight of **1** by one mass unit. Zoomed-in MS spectra of reaction with H_2O (top) and D_2O (bottom) are shown above the structure of 3-^{2}H-**1**, the proposed placement of the ^{2}H atom based on the TiqS mechanism. See full NMR and GC−MS spectra in Figures S31−S33.

https://doi.org/10.1021/jacs.5c01828
J. Am. Chem. Soc. 2025, 147, 16293−16300

bicyclic diterpene analog of caryophyllene recently found from a soft coral TS,[15] and two 5/11-bicyclic dolabellatrienes, 3,7,18-dolabellatriene (**2**) and 3,7,10-dolabellatriene (**4**; SI, Figure 2B, Tables S5−S7, Figures S6−S19 and S21−S28). The relative and absolute configurations of **3** and **4** were determined by 2D NOESY analysis and vibrational circular dichroism[16−18] (VCD; SI, Figures S20 and S29). Diterpene **4** is reported here for the first time.

The 4/9-bicyclic **3**, originating via sequential or concerted 1,11- and 2,10-cyclization events and following the well-known mechanism of caryophyllene,[19] supports the proposal that the first step in the formation of **1** is the 1,11-cyclization of GGPP to **B2**$^+$ (Figure 3). The presence of two 5/11-bicyclic dolabellatrienes reveals the following step is 10,14-cyclization to **C**$^+$, a common second cyclization event seen in the biosynthesis of many di- and sesterterpenes.[20,21] The 9,10-alkene in **4**, also supports either a 1,3-hydride shift, or two sequential 1,2-hydride shifts, from C-10 to C-14 to yield **D**$^+$. The same initial steps are proposed for the formation of the tetraquinane skeleton in crinipellin biosynthesis;[14] however, the differences in the A and B rings of tetraisoquinane (Figure 1) necessitate a significant skeleton rearrangement from **D**$^+$ to yield **1**.

Deuterium Labeling Supports Rearrangements of Two Isoprene Units. To probe a potential skeletal rearrangement, we used ^{2}H-labeled GGPP to locate the isoprene units that form the A and B rings of **1**. Using the GGPP synthase CrtE, we biosynthesized 1,1-$^2H_2$-GGPP in situ with chemically synthesized 1,1-$^2H_2$-isopentenyl diphosphate (IPP) and FPP (Figure S30), and added TiqS. GC−MS analysis of the isotopically labeled **1** in the reaction with 1,1-$^2H_2$-GGPP displayed a molecular ion peak at m/z 273.2560 (Figure S33), signifying only one deuterium atom was retained during cyclization. The ^{1}H and ^{1}H−^{13}C HSQC spectra of ^{2}H-**1** was identical to **1** except the signal at H-1 (2.60 ppm) and correlation with C-1 (67.1 ppm) were absent (Figures 4A and S35); we renumbered the carbon skeleton of **1** based on the proposed cyclization mechanism in this study. Incubation of TiqS with chemically synthesized 1*R*-^{2}H-GGPP resulted in identical GC−MS and NMR data with that of 1,1-$^2H_2$-GGPP (Figure 4A), confirming the 1*R*-H of GGPP is retained and the 1*S*-H of GGPP is lost. The position of ^{1}H-1 suggested either multiple hydride or proton shifts or migration of C-1 to a bridgehead carbon of the B−C ring system. With the uncertainty of C-1 of the first isoprene unit, we designed an experiment using in situ generated 1,1,5,5-$^2H_4$-GGPP (Figure S30) to identify the position of the C-1 of the second isoprene unit (C-5 of **1**). GC−MS analysis revealed an m/z value of 275.2686 and NMR analysis showed the absence of three proton signals and three HSQC correlations in comparison with **1**: H-1 and H_2-5 (Figures 4A and S31−S33). In addition, GC−MS analysis of deuterium-labeled **4** and **10** from these reactions (Figures S34 and S35) support the proposal that the 1*S*-H of GGPP is lost after intermediate **D**$^+$ is formed. These results suggested the fragmentation of two isoprene units in the cyclization of **1** and deprotonation of the pro-*S* hydrogen on C-1.

Site-Directed Mutation in the Active Site Reveals Key Residues Controlling the Cyclization Cascade. With the propensity of TiqS to form multiple products, we envisioned that altering the active site of TiqS may lead to additional shunt pathway products, as is common for many TSs,[20] that would give insight into key intermediates in the pathway to **1**. To identify residues of interest for mutation, we utilized sequence alignments with two highly homologous, but uncharacterized, TSs from *Cystobacter ferrugineus* (Figure S36) and Alphafold[22] and Autodock[23] to obtain a model of GGPP bound to TiqS (Figure S37). A total of 25 TiqS variants were produced, purified, and tested for diterpene cyclase activity (Figures 2 and S38−S41). TiqS possesses Asp-rich motifs ^{84}DDxxA and ^{223}NxxxSxxxD, as well as the commonly conserved ^{316}RY pair. TiqS variants D84A, D84E, D85A, R316 K, and R316H were either completely or nearly inactive, supporting their expected importance in type I TS activity. Although there are growing numbers of examples of functional TSs with modified DDxxD motifs,[6,19] we were interested in the importance of A88. Reinstalling the canonical DDxxD motif with the A88D variant significantly decreased the production of **1** and other products, but its counterpart A88E was active with a product distribution similar to that of native TiqS. Based on the docking model, W76, M77, F81, F151, and H311 form the active site contour and were proposed to interact with cationic intermediates. Only variants M77A, F151Y, H311W, and H311Y were completely inactive. Several variants produced new diterpenes or increased the yield of minor products seen in wild-type TiqS, which allowed their isolation and structural characterization. (Figure 2). F81 and W76 are key residues controlling product distribution in TiqS: removal of the aromaticity in F81A and F81L decreased the yield of **1** while still producing **2**−**4** and several new peaks; F81L/Y/W and W76L/Y/F/H increased the production of diterpenes **6**−**10**. Products **5** and **6**, isolated from F81A, were determined to be the known diterpenes *β*-springene and 3,7,11-dolabellatriene (SI, Figure 2, Tables S8 and S9 and Figures S42−S48). EIMS and NMR analysis of **7** and **8**, isolated from F81L, revealed that they are novel tricyclic skeletons with a fused 5/6-bicycle with a pendant cyclopentenyl moiety (SI, Figure 2, Tables S10 and S11 and Figures S49−S64); **7** and **8** were named secovulgarisenes A and B, respectively, given their proposed biosynthetic origin (see below) and their structural similarity to 11-hydroxyvulgarisane, the product of the plant TS PvHVS[24] (Figure S1). The relative configuration of **8** was determined by 2D NOESY analysis and VCD (SI, Figure S65). Products **9** and **10**, isolated from F81Y and W76L, respectively, are tetraisoquinene isomers with their alkenes positioned at 3(20) and 2(6) (SI, Figure 2, Tables S12 and S13 and Figures S66−S82).

Several key cationic intermediates in the cyclization of **1** are supported by the structures of **5**−**10** (Figure 3). Intermediates **A**$^+$ and **D**$^+$ yield **5** and **6**, respectively, via final shunt pathway deprotonation. Given the position of Me-18 on **1** (C-10), a 1,2-methyl shift is required and moving Me-18 from C-11 to C-10 from from **D**$^+$ yields **E**$^+$. The novel skeletons of **7** and **8** are consistent with the 5/6/5/5-tetracyclic secondary cation **J**$^+$, as a ring opening deprotonation at C-6 would provide **8**. An alternate 1,2-alkyl shift from **J**$^+$, with the shared electrons from the C-7/C-8 bond, affords the final proposed cation **K**$^+$, where deprotonation at C-6 yields **1** and off-pathway hydride shifts and deprotonations yield **9** and **10**. Carbocation **J**$^+$ is hypothesized to result from a 1,2-alkyl shift of the 5/6/4/5-tetracyclic **I**$^+$ (another possible direct precursor of **7** and **8**), which can be accessed from a 1(11),2,6-dolabellatriene neutral intermediate (**F**) via reprotonation at C-3 (**G**$^+$) and sequential 2,6- (**H**$^+$) and 1,7-cyclizations. Deprotonation of **E**$^+$ at C-1 affords **F** and would explain the loss of the 1*S*-H of GGPP in

https://doi.org/10.1021/jacs.5c01828
J. Am. Chem. Soc. 2025, 147, 16293−16300

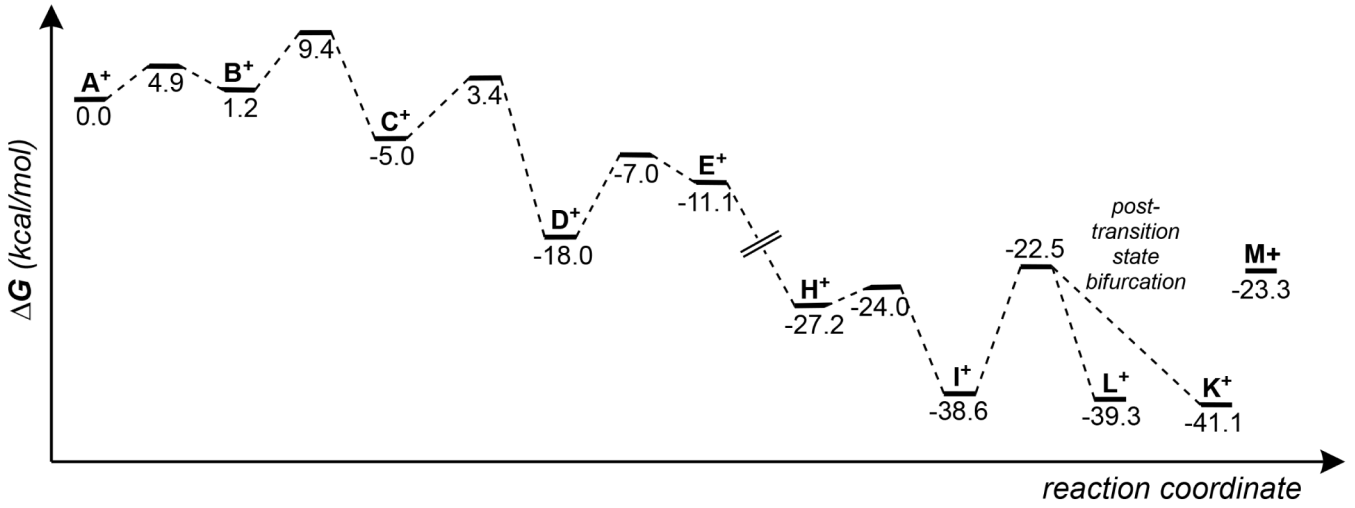

Figure 5. Energetics for the proposed carbocation cascade. Relative free energies of carbocations computed at the mPW1PW91/6-31+G(d,p) level of theory.

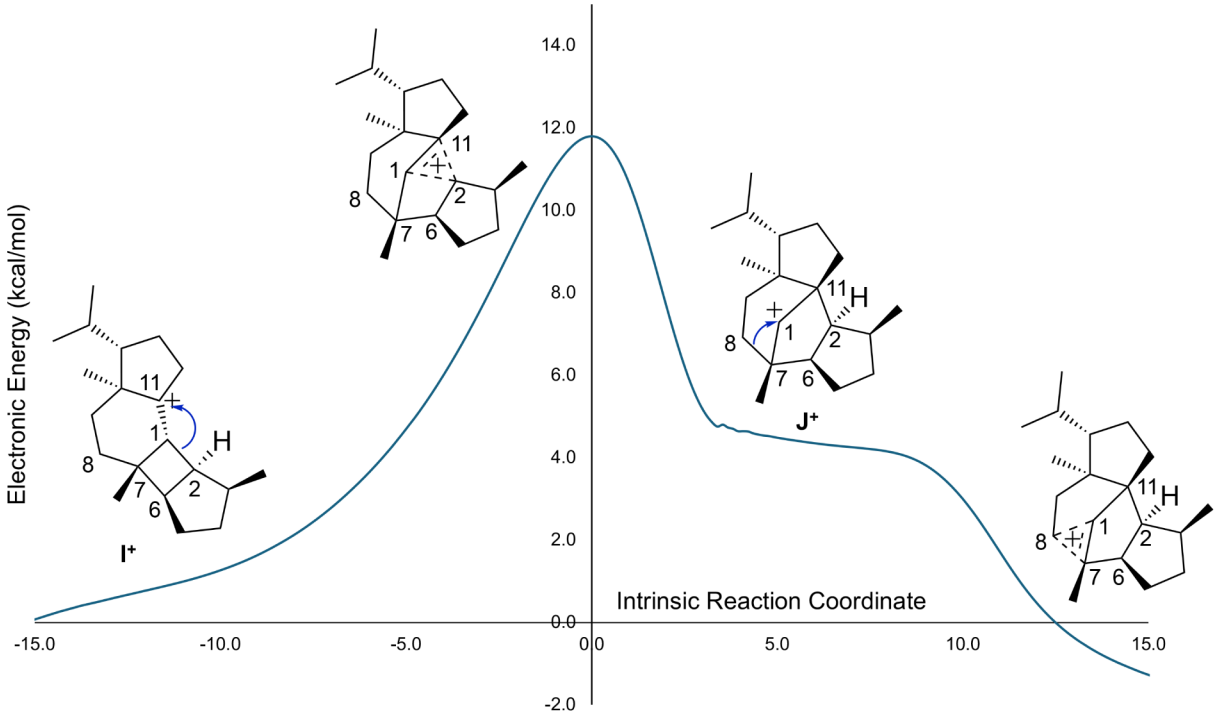

Figure 6. Intrinsic reaction coordinate for conversion of I^+ to K^+. Relative electronic (potential) energies computed at the mPW1PW91/6-31+G(d,p) level of theory.

the earlier described deuterium labeling experiments. This mechanism is fully consistent with the formation of **1**−**10**.

DFT Quantum Chemical Calculations Support the Proposed Cyclization Mechanism and Reveal a Post-Transition State Bifurcation. To help elucidate an energetically viable cyclization pathway, we performed quantum chemical calculations.[25−27] Relative free energies of the intermediates and transition structures (Figure 5) were computed at the mPW1PW91/6-31+G(d,p) level,[28−32] which has been previously validated for terpene-forming carbocation reactions.[27,33] The overall cationic cascade in Figure 3 flows downhill in free energy, with K^+ predicted to be 41 kcal mol^{-1} lower in free energy than A^+. While the first step was proposed to be 1,11-cyclization based on isolation of **3**, we did not find a transition state for direct 1,11-cyclization and propose an initial 1,10-cyclization to B^+ followed by a concerted 1,2-alkyl shift and 10,14-cyclization to yield C^+ (Figure 3). A dolabellyl cation is proposed to form from the geranylgeranyl cation via barrier-less and concerted 1,11- and 10,14-ring closures in the CotB2 mechanism;[34] while a similar path is possible here, we were unable to locate such a concerted ring closure to C^+. The only intermediate along the $A^+ \rightarrow K^+$ pathway that is higher in free energy than its preceding intermediate is E^+ (+6.9 kcal mol^{-1}), which is formed via a 1,2-methyl shift predicted to be accompanied by a barrier of 11 kcal mol^{-1}. The most energetically taxing step is the formation of K^+ from I^+ (barrier of 16.1 kcal mol^{-1}). Note that secondary carbocation J^+ was found not to be an

https://doi.org/10.1021/jacs.5c01828
J. Am. Chem. Soc. 2025, 147, 16293−16300

intermediate in this process. Instead, the computed reaction coordinate connecting $\mathbf{K}^+$ to $\mathbf{I}^+$ involves only a single transition structure (Figure 6). Structures resembling $\mathbf{J}^+$ are found along this reaction coordinate, but at the shoulder after the transition structure; however, these involve significant delocalization via hyperconjugation.[35] The presence of this shoulder hinted that the $\mathbf{I}^+$ to $\mathbf{K}^+$ transition structure might be followed by a post-transition state bifurcation;[36−40] i.e., a pathway downhill in free energy that splits, allowing two products to form from a single transition state. To test that hypothesis, ab initio molecular dynamics simulations were run,[41−43] and these revealed that both products $\mathbf{K}^+$ (7/8-bond cleavage) and $\mathbf{L}^+$ (10,11-bond cleavage) could be accessed from the $\mathbf{I}^+$ to $\mathbf{K}^+$ transition state (Figure S83). Formation of the latter in only a small amount (1:10) is consistent with the experimental observation of **1** as the major product and hints that this selectivity may involve nonstatistical dynamic effects inherent to the carbocation substrates.[44,45] A third option, 2,11-bond cleavage, would yield the 5/6−5 tricyclic secondary cation $\mathbf{M}^+$, but this intermediate is slightly lower in free energy than the transition structure and therefore higher in free energy than $\mathbf{J}^+$. The pathway through $\mathbf{M}^+$ (Figure 3), however, is possible in several TiqS variants (e.g., F81L) where the electronic contour of the active site may guide the cascade through minor pathways.

Another unusual feature of the mechanism shown in Figure 3 is the $\mathbf{E}^+ \rightarrow \mathbf{F} \rightarrow \mathbf{G}^+$ deprotonation/reprotonation sequence. This process was suggested because no carbocation-only process with reasonable energetic barriers for conversion of $\mathbf{E}^+$ to $\mathbf{G}^+$ (or any subsequent carbocation) could be found. While deprotonation/reprotonation processes are well precedented in terpene biosynthesis, what makes this one unusual is that we believe it may involve the released pyrophosphate (OPP^-) base;OPP^- has been suggested as the final base in other systems.[46−48] This contention derives from the fact that OPP was initially attached to C-1 and deprotonation is proposed to occur on this same carbon. After initial OPP^- loss, the positive charge on the carbon skeleton migrates away from OPP^- as the first few intermediates are formed. But when it returns to the neighborhood of OPP^- it can potentially be "quenched" by deprotonation. However, reprotonation can then lead to a subsequent carbocation cascade that is thermodynamically favorable. Note that carbocation $\mathbf{G}^+$ also is not predicted to be a discrete intermediate; the proximity of C-2 (carbocation center) and C-6 (π-bond) lead to a barrierless cyclization reaction.

TiqS in D_2O Supports the Presence of a Dolabellatriene Neutral Intermediate. To probe the presence of the neutral intermediate **F**, and therefore the necessary deprotonation and reprotonation events, in TiqS catalysis, TiqS was incubated with GGPP in D_2O buffer. GC−MS analysis of **1** produced in this reaction displayed a molecular ion peak at m/z 273.2532, representative of an M^+ ion containing a single deuterium atom (Figures 4B and S31). This result, along with the loss of the pro-*S* hydrogen at C-1 during catalysis, strongly implicates that 1(11),2,6-dolabellatriene (**F**) is in fact a true intermediate. The incorporation of a deuterium from an ionizable functional group on TiqS or directly from D_2O shows that reprotonation at C-3 does not involve the same proton lost when forming **F**.

CONCLUSIONS

Terpenoids are high value natural products and the characterization of new skeletons promises advances in natural product discovery, TS enzymology, biocatalysis, and organic chemistry. Although the majority of known terpenoids are from plants, fungi, and marine invertebrates, bacteria have proven to be a rich reservoir of uncharacterized terpenoid biosynthetic enzymes and new terpene skeletons. Myxobacteria are a quintessential example of this; they are well-known producers of diverse secondary metabolites[49] but only a few terpenoids are known[50] from this phylum. Several peptidic natural products are known from *M. boletus* DSM 148713,[51−53] but its genome displays impressive biosynthetic potential. The identification via genome mining and characterization of TiqS and its novel 5/5/5/5 tetraisoquinane skeleton from *M. boletus* supports this notion. We are currently focused on identifying the natural product generated by a hypothetical biosynthetic gene cluster encoding TiqS and evaluating its potential biological activity and ecological function.

TiqS catalyzes a complex cyclization cascade ultimately yielding the tetraisoquinane skeleton. We propose a reasonable mechanism using a combination of shunt products, mutagenesis, isotope labeling, and data from quantum chemical computations. The mechanism entails a dolabellatriene neutral intermediate and a unique rearrangement of two isoprene units through a concerted rearrangement that avoids a discrete secondary carbocation and opens up a post-transition state bifurcation. TiqS was particularly flexible in regard to product formation yielding five different carbon skeletons, which was an important attribute that led to the mechanistic proposal. Detailed structural analysis of TiqS is required to fully understand its catalysis and will lead to opportunities in TS engineering. Overall, the complexity and novelty of TiqS cyclization implies that myxobacteria produce new skeletons and terpenoid discovery awaits.

ASSOCIATED CONTENT

Data Availability Statement

All data generated or analyzed in this study are available within the article and its Supporting Information. Plasmids generated in this study will be provided upon request. The raw NMR data **1**−**10** were deposited in the Natural Product Magnetic Resonance Database (NP-MRD) under accession numbers NP0341974−NP0341982 (**1**−**4**, **6**−**10**) and NP0064998 (**5**). Mass spectra data of diterpenes were submitted to the Mass Spectra for Chemical Ecology (MACE) repository and will be made available upon its next release. A data set collection of computation results is available in the IoChem-BD repository at https://doi.org/10.19061/iochem-bd-6-423.

Supporting Information

The Supporting Information is available free of charge at https://pubs.acs.org/doi/10.1021/jacs.5c01828.

Experimental methods, strains, plasmids, and primers, spectroscopic data (EIMS, NMR, VCD) for **1**−**10**, supporting HPLC and GC−MS chromatograms of TiqS, variant, and labeling experiments, bioinformatics, and additional MD simulations (PDF)

VCD calculations (PDF)

AUTHOR INFORMATION

Corresponding Authors

Jeffrey D. Rudolf − *Department of Chemistry, University of Florida, Gainesville, Florida 32611-7011, United States;* orcid.org/0000-0003-2718-9651; Email: jrudolf@chem.ufl.edu

https://doi.org/10.1021/jacs.5c01828
J. Am. Chem. Soc. 2025, 147, 16293−16300

Dean J. Tantillo − *Department of Chemistry, University of California−Davis, Davis, California 95616, United States;* orcid.org/0000-0002-2992-8844; Email: djtantillo@ucdavis.edu

Authors

Xiuting Wei − *Department of Chemistry, University of Florida, Gainesville, Florida 32611-7011, United States*

William DeSnoo − *Department of Chemistry, University of California−Davis, Davis, California 95616, United States*

Zining Li − *Department of Chemistry, University of Florida, Gainesville, Florida 32611-7011, United States;* Present Address: Department of Biopharmaceutics, West China School of Pharmacy, Sichuan University, Chengdu, 610041, PR China; Key Laboratory of Drug-Targeting and Drug Delivery System of the Education Ministry and Sichuan Province, Sichuan Engineering Laboratory for Plant-Sourced Drug and Sichuan Research Center for Drug Precision Industrial Technology, West China School of Pharmacy, Sichuan University, Chengdu, 610041, China; orcid.org/0000-0002-6921-8417

Wenbo Ning − *Department of Chemistry, University of Florida, Gainesville, Florida 32611-7011, United States*

Wang-Yeuk Kong − *Department of Chemistry, University of California−Davis, Davis, California 95616, United States;* orcid.org/0000-0002-4592-0666

Jordan Nafie − *BioTools, Inc., Gainesville, Florida 33407, United States*

Complete contact information is available at: https://pubs.acs.org/10.1021/jacs.5c01828

Notes

The authors declare no competing financial interest.

■ ACKNOWLEDGMENTS

This work is supported in part by the National Institutes of Health Grant R35 GM142574 and the University of Florida (to J.D.R.) and the National Institutes of Health Grant R35 GM153469, along with computational support from the NSF ACCESS program (to D.J.T.). We thank the University of Florida Mass Spectrometry Research and Education Center, which is supported by the NIH (S10 OD021758-01A1) and Katie Heiden for GC−MS support. We thank the University of Florida Center for Nuclear Magnetic Resonance Spectroscopy and the University of Florida McKnight Brain Institute at the National High Magnetic Field Laboratory's Advanced Magnetic Resonance Imaging and Spectroscopy (AMRIS) Facility, which is supported by the US NSF Cooperative Agreement no. DMR-2128556 and the State of Florida, for NMR support. Special thanks to Drs. James Rocca and Ion Ghiviriga for NMR support. We acknowledge Tyler Alsup and Daniel Icenhour for design and construction of the MKI5 plasmid.

■ REFERENCES

(1) *Dictionary of Natural Products*. https://dnp.chemnetbase.com. Accessed 15 August 2024.

(2) Yan, Y.; Liu, Q.; Zang, X.; Yuan, S.; Bat-Erdene, U.; Nguyen, C.; Gan, J.; Zhou, J.; Jacobsen, S. E.; Tang, Y. Resistance-Gene-Directed Discovery of a Natural-Product Herbicide with a New Mode of Action. *Nature* **2018**, *559* (7714), 415−418.

(3) Avalos, M.; Garbeva, P.; Vader, L.; Wezel, G. P.; Dickschat, J. S.; Ulanova, D. Biosynthesis, Evolution and Ecology of Microbial Terpenoids. *Nat. Prod. Rep.* **2022**, *39* (2), 249−272.

(4) Huang, M.; Lu, J.-J.; Huang, M.-Q.; Bao, J.-L.; Chen, X.-P.; Wang, Y.-T. Terpenoids: Natural Products for Cancer Therapy. *Expert Opin. Invest. Drugs* **2012**, *21* (12), 1801−1818.

(5) Mewalal, R.; Rai, D. K.; Kainer, D.; Chen, F.; Külheim, C.; Peter, G. F.; Tuskan, G. A. Plant-Derived Terpenes: A Feedstock for Specialty Biofuels. *Trends Biotechnol.* **2017**, *35* (3), 227−240.

(6) Wei, X.; Ning, W.; McCadden, C. A.; Alsup, T. A.; Li, Z.; Łomowska-Keehner, D. P.; Nafie, J.; Qu, T.; Opoku, M. O.; Gillia, G. R.; Xu, B.; Icenhour, D. G.; Rudolf, J. D. Exploring and Expanding the Natural Chemical Space of Bacterial Diterpenes. *Nat. Commun.* **2025**, *16*, 3721.

(7) Kupka, J.; Anke, T.; Oberwinkler, F.; Schramm, G.; Steglich, W. Antibiotics from Basidiomycetes. VII. Crinipellin, a New Antibiotic from the Basidiomycetous Fungus *Crinipellis Stipitaria* (Fr.) Pat. *J. Antibiot. (Tokyo)* **1979**, *32* (2), 130−135.

(8) Anke, T.; Heim, J.; Knoch, F.; Mocek, U.; Steffan, B.; Steglich, W. Crinipellins, the First Natural Products with a Tetraquinane Skeleton. *Angew. Chem., Int. Ed.* **1985**, *24* (8), 709−711.

(9) Piers, E.; Renaud, J. Total Synthesis of the Tetraquinane Diterpenoid (+-)-Crinipellin B. *J. Org. Chem.* **1993**, *58* (1), 11−13.

(10) Piers, E. Tetraquinane Diterpenoids: Total Synthesis of (±)-Crinipellin B. *Synthesis* **1998**, *1998* (Sup. 1), 590−602.

(11) Kang, T.; Song, S. B.; Kim, W.-Y.; Kim, B. G.; Lee, H.-Y. Total Synthesis of (−)-Crinipellin A. *J. Am. Chem. Soc.* **2014**, *136* (29), 10274−10276.

(12) Huang, Z.; Huang, J.; Qu, Y.; Zhang, W.; Gong, J.; Yang, Z. Total Syntheses of Crinipellins Enabled by Cobalt-Mediated and Palladium-Catalyzed Intramolecular Pauson−Khand Reactions. *Angew. Chem., Int. Ed.* **2018**, *57* (28), 8744−8748.

(13) Zhao, Y.; Hu, J.; Chen, R.; Xiong, F.; Xie, H.; Ding, H. Divergent Total Syntheses of (−)-Crinipellins Facilitated by a HAT-Initiated Dowd−Beckwith Rearrangement. *J. Am. Chem. Soc.* **2022**, *144* (6), 2495−2500.

(14) Xu, B.; Zhang, Z.; Tantillo, D. J.; Dai, M. Concise Total Syntheses of (−)-Crinipellins A and B Enabled by a Controlled Cargill Rearrangement. *J. Am. Chem. Soc.* **2024**, *146* (31), 21250−21256.

(15) Burkhardt, I.; de Rond, T.; Chen, P. Y.-T.; Moore, B. S. Ancient Plant-like Terpene Biosynthesis in Corals. *Nat. Chem. Biol.* **2022**, *18* (6), 664−669.

(16) Nafie, L. A.; Dukor, R. K.; Freedman, T. B.Vibrational circular dichroism. In: Chalmers JM, Griffiths PR *Handbook of Vibrational Spectroscopy*; Wiley: Chichester, 2002. pp. 731−744.

(17) He, Y.; Bo, W.; Dukor, R. K.; Nafie, L. A. Determination of Absolute Configuration of Chiral Molecules Using Vibrational Optical Activity. *A Review. Appl. Spectrosc.* **2011**, *65* (7), 699−723.

(18) Klein Hendges, A. P. P.; dos Santos, E. F.; Teixeira, S. D.; Santana, F. S.; Trezzi, M. M.; Batista, A. N. L.; Batista, J. M., Jr; de Lima, V. A.; de Assis Marques, F.; Maia, B. H. L. N. S. Phytotoxic Neocassane Diterpenes from Eragrostis Plana. *J. Nat. Prod.* **2020**, *83* (12), 3511−3518.

(19) Dickschat, J. S. Bacterial Terpene Cyclases. *Nat. Prod. Rep.* **2016**, *33* (1), 87−110.

(20) Tomita, T.; Kim, S.-Y.; Teramoto, K.; Meguro, A.; Ozaki, T.; Yoshida, A.; Motoyoshi, Y.; Mori, N.; Ishigami, K.; Watanabe, H.; Nishiyama, M.; Kuzuyama, T. Structural Insights into the CotB2-Catalyzed Cyclization of Geranylgeranyl Diphosphate to the Diterpene Cyclooctat-9-En-7-Ol. *ACS Chem. Biol.* **2017**, *12* (6), 1621−1628.

(21) Rinkel, J.; Lauterbach, L.; Dickschat, J. S. A Branched Diterpene Cascade: The Mechanism of Spinodiene Synthase from *Saccharopolyspora spinosa*. *Angew. Chem., Int. Ed.* **2019**, *58* (2), 452−455.

(22) Jumper, J.; Evans, R.; Pritzel, A.; Green, T.; Figurnov, M.; Ronneberger, O.; Tunyasuvunakool, K.; Bates, R.; Žídek, A.; Potapenko, A.; Bridgland, A.; Meyer, C.; Kohl, S. A. A.; Ballard, A.

J.; Cowie, A.; Romera-Paredes, B.; Nikolov, S.; Jain, R.; Adler, J.; Back, T.; Petersen, S.; Reiman, D.; Clancy, E.; Zielinski, M.; Steinegger, M.; Pacholska, M.; Berghammer, T.; Bodenstein, S.; Silver, D.; Vinyals, O.; Senior, A. W.; Kavukcuoglu, K.; Kohli, P.; Hassabis, D. Highly Accurate Protein Structure Prediction with AlphaFold. *Nature* **2021**, *596* (7873), 583−589.
(23) Forli, S.; Huey, R.; Pique, M. E.; Sanner, M. F.; Goodsell, D. S.; Olson, A. J. Computational Protein−Ligand Docking and Virtual Drug Screening with the AutoDock Suite. *Nat. Protoc.* **2016**, *11* (5), 905−919.
(24) Johnson, S. R.; Bhat, W. W.; Sadre, R.; Miller, G. P.; Garcia, A. S.; Hamberger, B. Promiscuous Terpene Synthases from Prunella Vulgaris Highlight the Importance of Substrate and Compartment Switching in Terpene Synthase Evolution. *New Phytol.* **2019**, *223* (1), 323−335.
(25) Tantillo, D. J. Interrogating Chemical Mechanisms in Natural Products Biosynthesis Using Quantum Chemical Calculations. *Wiley Interdiscip. Rev.: comput. Mol. Sci.* **2020**, *10* (3), No. e1453.
(26) Tantillo, D. J. 1.20 - Exploring Terpenoid Biosynthesis With Quantum Chemical Computations. *In Comprehensive Natural Products III; Liu, H.-W. (Ben)*, Begley, T. P. 1.20 - Exploring Terpenoid Biosynthesis With Quantum Chemical Computations. In *In Comprehensive Natural Products III; Liu, H.-W. (Ben)*; Elsevier: Oxford, 2020, pp. 644−653. .
(27) Tantillo, D. J. Biosynthesis via Carbocations: Theoretical Studies on Terpene Formation. *Nat. Prod. Rep.* **2011**, *28* (6), 1035−1053.
(28) Adamo, C.; Barone, V. Exchange Functionals with Improved Long-Range Behavior and Adiabatic Connection Methods without Adjustable Parameters: The mPW and mPW1PW Models. *J. Chem. Phys.* **1998**, *108* (2), 664−675.
(29) Clark, T.; Chandrasekhar, J.; Spitznagel, G. W.; Schleyer, P. V. R. Efficient Diffuse Function-Augmented Basis Sets for Anion Calculations. III. The 3−21+G Basis Set for First-Row Elements, Li−F. *J. Comput. Chem.* **1983**, *4* (3), 294−301.
(30) Ditchfield, R.; Hehre, W. J.; Pople, J. A. Self-Consistent Molecular-Orbital Methods. IX. An Extended Gaussian-Type Basis for Molecular-Orbital Studies of Organic Molecules. *J. Chem. Phys.* **1971**, *54* (2), 724−728.
(31) Hariharan, P. C.; Pople, J. A. The Influence of Polarization Functions on Molecular Orbital Hydrogenation Energies. *Theor. Chim. Acta.* **1973**, *28* (3), 213−222.
(32) Hehre, W. J.; Ditchfield, R.; Pople, J. A. Self—Consistent Molecular Orbital Methods. XII. Further Extensions of Gaussian—Type Basis Sets for Use in Molecular Orbital Studies of Organic Molecules. *J. Chem. Phys.* **1972**, *56* (5), 2257−2261.
(33) Matsuda, S. P. T.; Wilson, W. K.; Xiong, Q. Mechanistic Insights into Triterpene Synthesis from Quantum Mechanical Calculations. Detection of Systematic Errors in B3LYP Cyclization Energies. *Org. Biomol. Chem.* **2006**, *4* (3), 530−543.
(34) Raz, K.; Driller, R.; Dimos, N.; Ringel, M.; Brück, T.; Loll, B.; Major, D. T. The Impression of a Nonexisting Catalytic Effect: The Role of CotB2 in Guiding the Complex Biosynthesis of cyclooctat-9-en-7-ol. *J. Am. Chem. Soc.* **2020**, *142* (51), 21562−21574.
(35) Tantillo, D. J. The Carbocation Continuum in Terpene Biosynthesis—Where Are the Secondary Cations? *Chem. Soc. Rev.* **2010**, *39* (8), 2847−2854.
(36) Ess, D. H.; Wheeler, S. E.; Iafe, R. G.; Xu, L.; Çelebi-Ölçüm, N.; Houk, K. N. Bifurcations on Potential Energy Surfaces of Organic Reactions. *Angew. Chem., Int. Ed.* **2008**, *47* (40), 7592−7601.
(37) Hare, S. R.; Tantillo, D. J. Post-Transition State Bifurcations Gain Momentum − Current State of the Field. *Pure Appl. Chem.* **2017**, *89* (6), 679−698.
(38) Carpenter, B. K. Energy Disposition in Reactive Intermediates. *Chem. Rev.* **2013**, *113* (9), 7265−7286.
(39) Rehbein, J.; Wulff, B. Chemistry in Motion—off the MEP. *Tetrahedron Lett.* **2015**, *56* (50), 6931−6943.
(40) Tantillo, D. J. Chapter One - Beyond Transition State Theory—Non-Statistical Dynamic Effects for Organic Reactions. *In Advances in Physical Organic Chemistry*; Williams, I. H.; Williams, N. H. Chapter One - Beyond Transition State Theory—Non-Statistical Dynamic Effects for Organic Reactions. In *In Advances in Physical Organic Chemistry*; Academic Press, 2021, Vol. *55*, pp. 1−16. .
(41) Jayee, B.; Hase, W. L. Nonstatistical Reaction Dynamics. *Annu. Rev. Phys. Chem.* **2020**, *71*, 289−313.
(42) Carpenter, B. K. Nonstatistical Dynamics in Thermal Reactions of Polyatomic Molecules. *Annu. Rev. Phys. Chem.* **2005**, *56*, 57−89.
(43) Teynor, M. S.; Wohlgemuth, N.; Carlson, L.; Huang, J.; Pugh, S. L.; Grant, B. O.; Hamilton, R. S.; Carlsen, R.; Ess, D. H. *Milo, Revision 1.0.3*; Brigham Young University: Provo UT, 2021.
(44) Tantillo, D. J. Importance of Inherent Substrate Reactivity in Enzyme-Promoted Carbocation Cyclization/Rearrangements. *Angew. Chem., Int. Ed.* **2017**, *56* (34), 10040−10045.
(45) Hare, S. R.; Tantillo, D. J. Dynamic Behavior of Rearranging Carbocations − Implications for Terpene Biosynthesis. *Beilstein J. Org. Chem.* **2016**, *12* (1), 377−390.
(46) Major, D. T.; Weitman, M. Electrostatically Guided Dynamics—The Root of Fidelity in a Promiscuous Terpene Synthase? *J. Am. Chem. Soc.* **2012**, *134* (47), 19454−19462.
(47) Ansbacher, T.; Freud, Y.; Major, D. T. Slow-Starter Enzymes: Role of Active-Site Architecture in the Catalytic Control of the Biosynthesis of Taxadiene by Taxadiene Synthase. *Biochemistry* **2018**, *57* (26), 3773−3779.
(48) Dixit, M.; Weitman, M.; Gao, J.; Major, D. T. Chemical Control in the Battle against Fidelity in Promiscuous Natural Product Biosynthesis: The Case of Trichodiene Synthase. *ACS Catal.* **2017**, *7* (1), 812−818.
(49) Wenzel, S. C.; Müller, R. Myxobacteria—'Microbial Factories' for the Production of Bioactive Secondary Metabolites. *Mol. BioSyst.* **2009**, *5* (6), 567−574.
(50) Rudolf, J. D.; Alsup, T. A.; Xu, B.; Li, Z. Bacterial Terpenome. *Nat. Prod. Rep.* **2021**, *38* (5), 905−980.
(51) Rukthanapitak, P.; Saito, K.; Kobayashi, R.; Kaweewan, I.; Kodani, S. Heterologous Production of a New Lanthipeptide Boletupeptin Using a Cryptic Biosynthetic Gene Cluster of the Myxobacterium *Melittangium Boletus*. *J. Biosci. Bioeng.* **2024**, *137* (5), 354−359.
(52) Thetsana, C.; Kobayashi, R.; Manadee, K.; Kodani, S. Isolation and Structure Determination of a New Depsipeptide Crocapeptin C from the Myxobacterium Melittangium Boletus. *Nat. Prod. Res.* **2024**, 1−7.
(53) Kaweewan, I.; Mukai, K.; Rukthanapitak, P.; Nakagawa, H.; Hosaka, T.; Kodani, S. Heterologous Biosynthesis of Myxobacterial Lanthipeptides Melittapeptins. *Appl. Microbiol. Biotechnol.* **2024**, *108* (1), 122.

https://doi.org/10.1021/jacs.5c01828
J. Am. Chem. Soc. 2025, 147, 16293−16300